Effect of flow disturbances remaining at the beginning of diastole on intraventricular diastolic flow and colour M-mode Doppler echocardiograms

M. Nakamura[1] S. Wada[1] T. Mikami[2] A. Kitabatake[3]
T. Karino[4] T. Yamaguchi[1]

[1]Graduate School of Engineering, Tohoku University, Japan
[2]College of Medical Technology, Hokkaido University, Japan
[3]Graduate School of Medicine, Hokkaido University, Japan
[4]Research Institute for Electronic Science, Hokkaido University, Japan

Abstract—*A computational model of the fluid dynamics of intraventricular flow was used to investigate the importance of the effects of flow disturbances existing within the left ventricle (LV) at the onset of diastole on a diastolic flow field. The simulation started with a quiescent flow state; it continued for a number of cardiac cycles to obtain a cyclically repeatable flow. After the flow became periodic, the initial diastolic flow was not quiescent: flow disturbances, remnants of a systolic flow, were present within the LV. Nevertheless, they faded away during an acceleration phase of diastole and almost ceased by the end of this phase. Consequently, a flow field during a deceleration phase of diastole, characterised by the formation of a vortex ring, was hardly affected by the initial flow disturbances. The propagation velocity of a colour M-mode Doppler echocardiogram obtained by scanning velocity along the LV long axis was 0.58 m s^{-1} in the case where diastolic flow was initially quiescent and 0.56 m s^{-1} in the case where flow disturbances existed at the beginning of diastole. These results indicated that the colour M-mode Doppler echocardiographic technique captures flow dynamics produced purely by ventricular expansion, with little influence from initial diastolic flow disturbances.*

Keywords—*Blood flow, Computational fluid dynamics, Left ventricle, Colour M-mode Doppler echocardiogram, Systole, Diastole*

Med. Biol. Eng. Comput., 2004, **42**, 509–515

1 Introduction

THE LEFT ventricle (LV) distributes blood to a systemic circulation by alternately contracting and expanding. Cardiac function is often evaluated from the viewpoint of contractility or systolic function. It is reported that its diastolic function, defined as the function to fill with blood without a compensatory increase in atrial filling pressures, also plays a key role in the blood pumping action (POLEUR *et al.*, 1989).

Recently, a novel method using colour motion-mode (M-mode) Doppler (CMD) echocardiography was proposed for assessing LV diastolic function (JACOBS *et al.*, 1990; STUGAARD *et al.*, 1994; MOLLER *et al.*, 2000). In this method, a velocity distribution along the LV long axis, spanning from the centre of a mitral valve orifice to a ventricular apex, is measured on the basis of a Doppler ultrasound technique. The measured velocity is presented in an M-mode image called a CMD echocardiogram. Evaluation of LV diastolic function is made based on a CMD echocardiogram colour pattern (DE MEY *et al.*, 2001).

Using computational fluid dynamics (CFD), we found that the CMD echocardiogram pattern is deeply involved with the development speed of a vortex ring rising in the LV during diastole (NAKAMURA *et al.*, 2001; 2002; 2003). These studies analysed the dynamics of intraventricular diastolic blood flow by assuming that blood flow was initially quiescent, as is commonly presumed in intraventricular flow simulation (TAYLOR and YAMAGUCHI, 1995; SABER *et al.*, 2001; 2003). However, an actual heart expands and contracts periodically. Flow is not at a standstill at the onset of diastole: there is remnant flow from the preceding systolic phase. In the initially quiescent flow condition, diastolic flow dynamics caused by the systolic flow disturbances that exist at the beginning of diastole cannot be analysed.

Correspondence should be addressed to Dr Masanori Nakamura; email: masanorin@pfsl.mech.tohoku.ac.jp

Paper received 9 October 2003 and in final form 3 February 2004
MBEC online number: 20043888

From a clinical point of view, investigation of the effects of initial flow disturbances on a diastolic flow field would aid in elucidating the applicability and limitations of CMD echocardiography. The present study examined the CFD of intraventricular blood flow for a series of cardiac cycles. Thereby, we examined the importance of flow disturbance effects that are incurred within the LV cavity at the onset of diastole on a diastolic flow field.

2 Methods

Simulations of intraventricular blood flow were carried out using the method we adopted in the previous study (NAKAMURA *et al.*, 2003). Here, we give an outline of the method.

2.1 *Configuration of an LV model at its maximum expansion*

Geometric information about the LV luminal surface in the long-axis plane was obtained from an image of a parasternal long-axis view of a human heart shown in a standard medical reference (HONMA *et al.*, 1998). Using it, we constructed an LV model. This configuration was adopted as the geometry of a fully expanded LV model. It was assumed that an LV is symmetric with respect to its common medium plane. A 10 mm long, straight conduit, with a radius equal to that of the mitral valve, was annexed onto the mitral valve as an entrance region; the top plane of the conduit was reassigned to the mitral valve. At this stage of design, the volume of the LV model was 117 cm^3. The distance from the mitral valve to the ventricular apex was 101 mm, the distance from the aortic valve to the ventricular apex was 86 mm, and the diameter of the mitral valve and the aortic valve was 26 mm. As shown in Fig. 1*a*, we regarded the LV as a tube bent like the letter 'U', having the mitral valve at one end and the aortic valve at the other end. We defined the cross-section Ψ that is obtained by cutting the LV with a plane radiated out from the line of intersection of the planes containing the two valve orifices.

2.2 *Construction of a computational model of the LV*

In each cross-sectional plane Ψ, a point O′ was set at the centroid of Ψ, as shown in Fig. 1*a*. Line *f* was defined as an intersection between Ψ and a symmetrical plane of LV; line *g* was a straight line that connected O′ with a point P on a circumference of Ψ. The angle between lines *f* and *g* was defined as θ, and the angle of Ψ from the plane of the mitral valve was introduced as α.

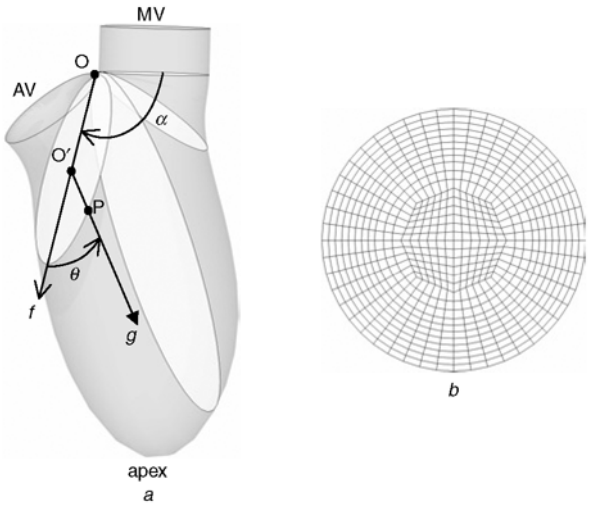

Fig. 1 *(a) Definitions of ψ,α and θ; (b) mesh of unit circle*

A unit circle model that had been divided into finite elements, as shown in Fig. 1*b*, was prepared to construct a computational model of an LV (481 nodes, 460 elements). Given an LV configuration, all cross-sections Ψ were replaced with this circle model after it was deformed so that its outline coincided with that of Ψ. A computational model of the LV was then produced by connecting corresponding nodal points between neighbouring cross-sections of Ψ to create a hexagonal element. The numbers of nodal points and elements were 24 531 and 23 000, respectively.

2.3 *Movement of the ventricular wall*

Two major assumptions were made for modelling ventricular wall movement. First, the ventricular wall motion was assumed to be independent of intraventricular pressure and flow. Secondly, a spatial distribution of the ventricular wall movement was fixed throughout a cardiac cycle. In addition, a point on the wall moved only in the direction of line *g*, that is, a line connecting the point itself and the centroid of cross-section Ψ on which the point existed.

With these assumptions, the relationship between the moving velocity of the ventricular wall v_w and a rate of volume change $dV(t)/dt$ at time t is given as

$$\frac{dV(t)}{dt} = \int\int_S v_w(t,\theta,\alpha)\boldsymbol{e}\cdot\boldsymbol{n}dS \tag{1}$$

where $\boldsymbol{e}$ is a unit vector in the direction of O′P, dS is the element of the area of the surface of the LV model, and $\boldsymbol{n}$ is a unit vector normal to the surface S. For simplicity, the moving velocity of the ventricular wall v_w was calculated as

$$v_w = v_a(t)W_1(\theta)W_2(\alpha) \tag{2}$$

where $v_a(t)$ is the moving velocity of a ventricular apex, and $W_1(\theta)$, $W_2(\alpha)$ are the weighting functions expressing the spatial distribution of a wall movement. If the weighting functions $W_1(\theta)$ and $W_2(\alpha)$ and the rate of volume change $dV(t)/dt$ are given, the velocity of the ventricular wall at any point and at any time can be calculated from (1) and (2).

2.4 *Conditions of a diastolic flow simulation*

Diastole consists of a phase of ventricular relaxation and a phase of atrial contraction. Nevertheless, because a CMD echocardiogram used for assessment of LV diastolic function is characterised by blood flow developing during the ventricular relaxation phase, this study simulated only that phase.

In the simulation of diastolic flow, the following weighting functions were used:

$$W_1(\theta) = \frac{1+\cos(\theta)}{2} \tag{3}$$

and

$$W_2(\alpha) = \frac{D(\alpha)-D(0)}{D_{max}-D(0)} \tag{4}$$

where $D(\alpha)$ is the length of the long axis of Ψ at an angle α at maximum expansion of the LV, and D_{max} is the maximum of $D(\alpha)$, which is obtained at $\alpha = 4\pi/9$ corresponding to the cross-section Ψ containing the ventricular apex. The weighting function $W_1(\theta)$ was given so that the moving velocity of point P on the wall decreased as it came closer to point O. The weighting function $W_2(\alpha)$ was set such that it maintained the radii of the mitral and aortic valves constant and maximised the velocity at the ventricular apex (NAKAMURA *et al.*, 2003).

Fig. 2 shows the time variation of the rate of the volume change $dV(t)/dt$ and the ventricular volume change $V(t)$ during diastole. Parameters were determined on the basis of clinical data

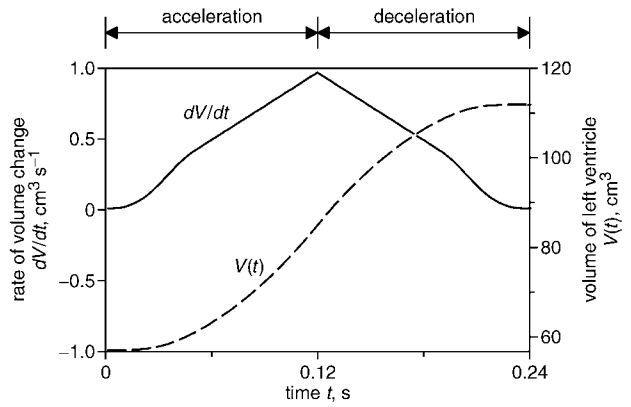

Fig. 2 *Time variation of (——) rate of LV volume change $dV(t)/dt$ and (-----) LV volume $V(t)$ during diastole*

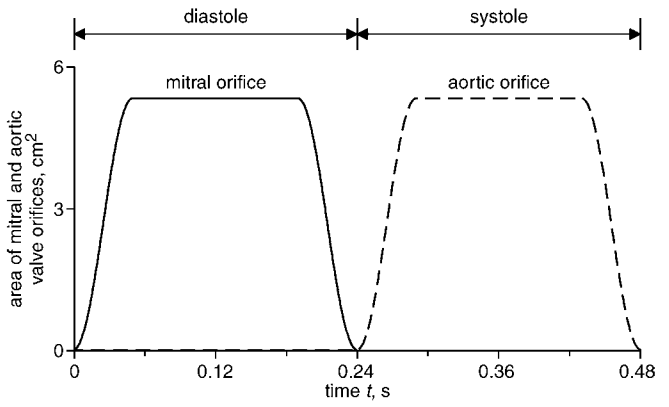

Fig. 3 *Time variation of areas of mitral and aortic orifices during cardiac cycle*

(KITABATAKE *et al.*, 1982). Times from the beginning of diastole ($t = 0$) to the peak $dV(t)/dt$ and to the end of diastole were set as 0.12 s and 0.24 s, respectively. Hereinafter, the former half of the diastole is referred to as an acceleration phase, during which $dV(t)/dt > 0$; the latter half is referred to as a deceleration phase. The net change in the volume was 55 cm^3.

2.5 *Conditions of systolic flow simulation*

Simulation of a systolic flow is intended to create flow disturbances at the beginning of diastole so that their effects on an actual diastolic flow can be investigated. Therefore, for simplicity, we used the same weighting functions of ventricular wall movements given in diastole for simulation of systolic flow. Furthermore, a temporal change in dV/dt during systole was given as a reversed process of dV/dt in diastole.

2.6 *Opening and closing of the mitral and aortic valves*

The mitral valve opens at the instant that expansion of LV is initiated. After remaining fully open for a short time, the mitral valve begins to close; the aortic valve is closed throughout diastole. In contrast, during systole, the aortic valve opens and closes with the mitral valve closed.

We modelled both valve orifices as a circular core. We then expressed opening and closing of the valve by varying the size of the core axisymmetrically from its center or its circumference with progression of expansion or contraction of LV. The importance of the valve orifice has been discussed by NAKAMURA *et al.* (2002). A change in the size of the valve orifice was described using trigonometric functions such that its time variation was C1-continuous (its first time derivative was zero). It was set such that full opening of the valve from a closed state took 0.05 s; the same time was required for complete closure from a fully opened state. Fig. 3 shows a plot of change in the areas of the mitral valve orifice and the aortic valve orifice as a function of time.

2.7 *Blood flow analysis*

Intraventricular blood flow was assumed to be a laminar flow in both systolic and diastolic phases. Blood was assumed to be a homogeneous and incompressible Newtonian fluid with $1.05 \times 10^3\,kg\,m^{-3}$ density and 3.5×10^{-3} Pa · s viscosity. The unsteady Navier–Stokes equations, along with the equation of continuity, were solved using a finite element method, implemented in a commercially available CFD code ANSYS-FLOTRAN version 5.6*. The boundary conditions applied for computing the blood velocity $\boldsymbol{U}$ and the blood pressure P during diastole were

$$\begin{aligned} P &= 0 && \text{on an opened part of the mitral and aortic valves} \\ \boldsymbol{U} &= 0 && \text{on a closed part of the mitral and aortic valves} \\ \boldsymbol{U} &= v_w \boldsymbol{e} && \text{on the ventricular wall} \end{aligned} \tag{5}$$

*Cybernet Systems Co. Ltd., Tokyo

2.8 *Computer simulation procedure*

Fig. 4 summarises the procedure of a computer simulation of intraventricular blood flow. The computer simulation of intraventricular flow began with diastole. The geometry of the LV model at the beginning of diastole was obtained from that at the maximum expansion by its volume being reduced by 60 ml. As an initial condition, blood in the LV was assumed to be quiescent. Advancing a time step, a time t was calculated simply by multiplying a time step with the increment of time Δt, which is 0.002 s. The rate of volume change of LV was then given according to the curve shown in Fig. 2. The moving velocity of the ventricular wall was calculated from (1) and (2) as v_w. Intraventricular blood flow was calculated using that velocity as a boundary condition.

After completion of CFD, the nodal points on the outer surface of LV were moved with the moving velocity of the ventricular wall calculated prior to the CFD. Updating of the geometry of the LV model was followed by remeshing. Physical quantities, namely velocity and pressure at new nodal points, were interpolated using Lagrange interpolation and data at surrounding nodal points defined at the previous time step. A numerical analysis of blood flow in the LV at a given time t was carried out repeating the above procedure. Systolic flow was simulated after the diastolic flow analysis had finished. This process was repeated until a fully cyclically repeating intraventricular flow was obtained.

3 Results

3.1 *Intraventricular flow in the initial cardiac cycle started with a quiescent flow*

Fig. 5 shows streamlines of intraventricular flow at five different moments during diastole of the initial cardiac cycle, where flow was at a standstill initially. The moments corresponding to the streamlines are

(*a*) the beginning of diastole
(*b*) the mid-point of an acceleration phase in dV/dt
(*c*) the peak of dV/dt
(*d*) the mid-point of a deceleration phase in dV/dt
(*e*) the end of diastole.

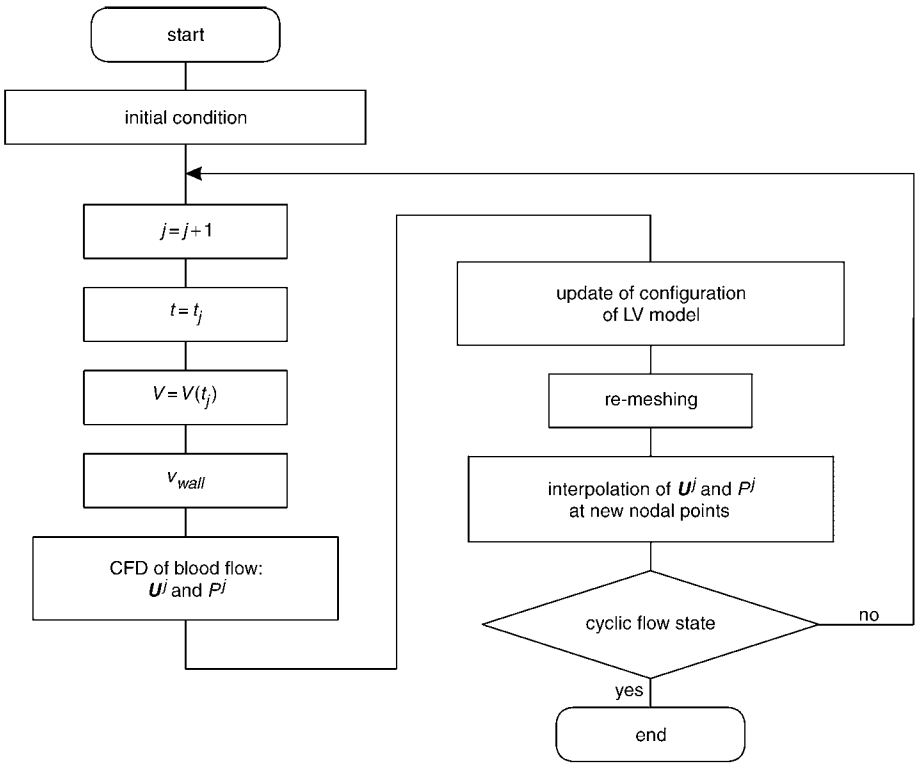

Fig. 4 *Flowchart of computer simulation procedure for intraventricular blood flow*

Images are viewed from the left of the LV, with its anterior side towards the left. The colour of the streamlines expresses the magnitude of velocity corresponding to a colour bar shown at the bottom of each Figure. At $t = 0$, the blood flow velocity was zero everywhere, as assumed in initial conditions (Fig. 5*a*). Ventricular filling was initiated with the onset of ventricular expansion. The blood that entred through the mitral orifice spread all over the intraventricular cavity, as shown in Fig. 5*b*. When an expansion rate changed from acceleration to deceleration, a clockwise rotating vortex was formed under the aortic valve, as in Fig. 5*c*. Although this vortex grew larger during the deceleration phase, it also extended in the lateral direction along the side wall of the LV, such that it encircled the blood flow along the LV long axis. Consequently, the vortex assumed a ringed structure that appeared as a pair of counter-rotating vortices located on each side of a fast, straight flow streaming along the long axis of the LV, as shown in Fig. 5*d*. Fig. 5*e* illustrates the state at the end of diastole: the annular vortex occupied a large space around a ventricular filling flow in the ventricular cavity, thereby constricting it. It was observed that a high-velocity point of blood inflow appeared on the long axis; it migrated from the level of the mitral valve to the middle of the ventricular cavity during diastole.

Blood was ejected from the aortic valve orifice during systole. As ventricular contraction progressed, the vortex under the aortic orifice, which was part of an annular vortex during diastole, diminished; conversely, the vortex on the posterior side grew larger and shifted to the LV apical region. At the end of systole, the vortex, which was originally a posterior part of the vortex ring, occupied a large space in the apical region (see Fig. 6*a*, described in the following Section).

3.2 *Intraventricular flow after a cyclically repeated pattern was obtained*

Blood flow assumed a cyclically repeating pattern through continuous computer simulations for some cardiac cycles. A repeatable flow field was obtained after four cardiac cycles. Fig. 6 shows blood flow in the LV during diastole in the fourth cardiac cycle. Moments in time of Figs 6*a–e* correspond to those in Fig. 5. Here also, all images are viewed from the left of the LV with its anterior side towards the left.

Intraventricular blood flow at the beginning of diastole was no longer quiescent: flow disturbances existed because of the preceding systolic phase. As shown in Fig. 6*a*, at that moment, blood flow was disturbed and a vortex that rotated counter-clockwise was seen in the region near the apex. This vortex obstructed blood inflow from the mitral orifice and prevented it from flowing straight towards the ventricular apex. Consequently, the blood inflow was directed towards the anterior side, and only a small portion of it went to the posterior side, (see Fig. 6*b*). With accelerated expansion of the LV, this vortex shrank and moved to the posterolateral region. At the transition from acceleration to the deceleration phase, a new vortex that rotated clockwise arose under the aortic orifice (Fig. 6*c*). Because of this new vortex, there were broadly two vortices in the LV cavity at that moment: one under the aortic valve, and the other in the posterolateral region. Whereas the vortex in the posterolateral region moved upward with further expansion of the LV, the vortex under the aortic valve extended circumferentially along the LV side wall to the posterior side and merged with the vortex that had travelled from the posterolateral region. Accordingly, as seen in Fig. 6*d*, one annular vortex surrounding blood inflow along the LV long axis was generated in the LV in the same manner as the one formed when the initial flow was quiescent. By the end of diastole, the flow pattern in the LV became macroscopically similar to the one seen in the first cardiac cycle, as shown in Fig. 6*e*.

3.3 *Colour M-mode Doppler echocardiogram of ventricular filling flow*

Fig. 7 shows spatiotemporal maps of the velocity distribution along the long axis of the LV obtained during diastole of the first–fourth cardiac cycles in our computation and plotted in the same manner as a CMD echocardiogram. In each map,

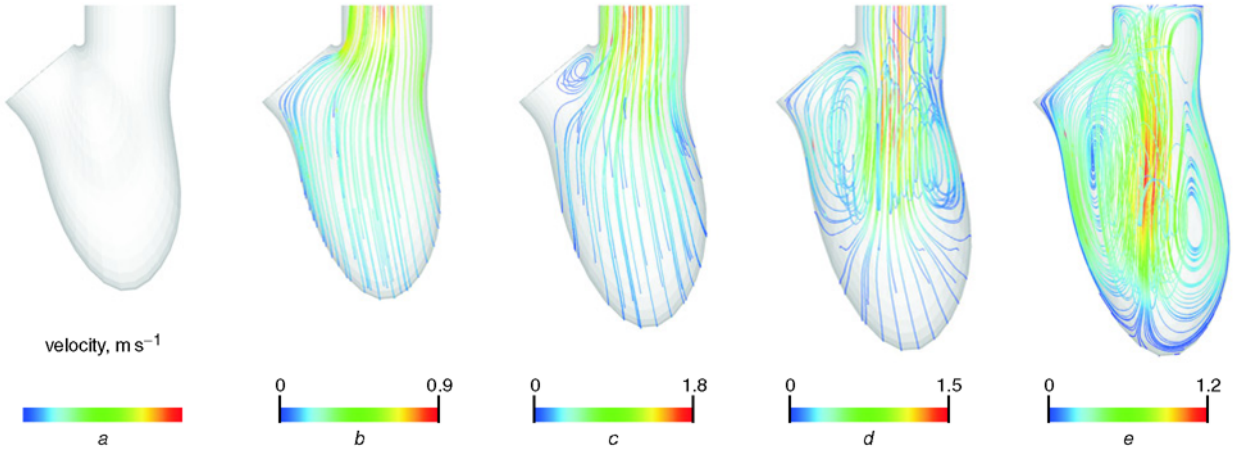

Fig. 5 *Streamlines of intraventricular diastolic flow during first cardiac cycle as observed normal to bisector plane of LV. Flow was quiescent at beginning of diastole of first cardiac cycle. (a) t = 0, at beginning of diastole; (b) t = 0.06 s, at mid-point in acceleration phase; (c) t = 0.12 s, at transition from acceleration to deceleration; (d) t = 0.18 s, at mid-point of deceleration phase; (e) t = 0.24 s, at end of diastole*

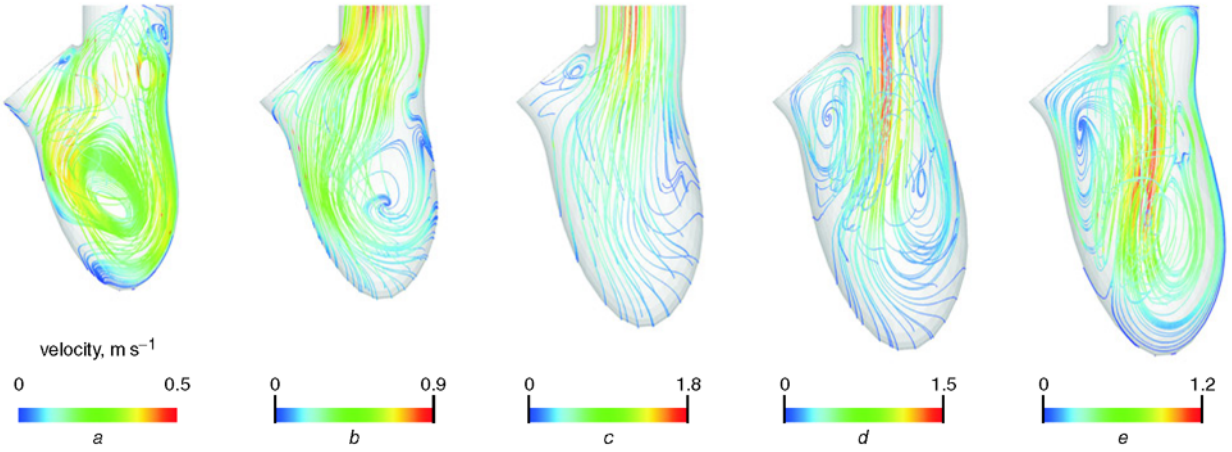

Fig. 6 *Streamlines of intraventricular diastolic flow during fourth cardiac cycle as observed normal to bisector plane of LV. Flow was not quiescent at beginning of diastole of this cardiac cycle. (a) t = 0, at beginning of diastole; (b) t = 0.06 s, at mid-point in acceleration phase; (c) t = 0.12 s, at transition from acceleration to deceleration; (d) t = 0.18 s, at mid-point in deceleration phase; (e) t = 0.24 s, at end of diastole*

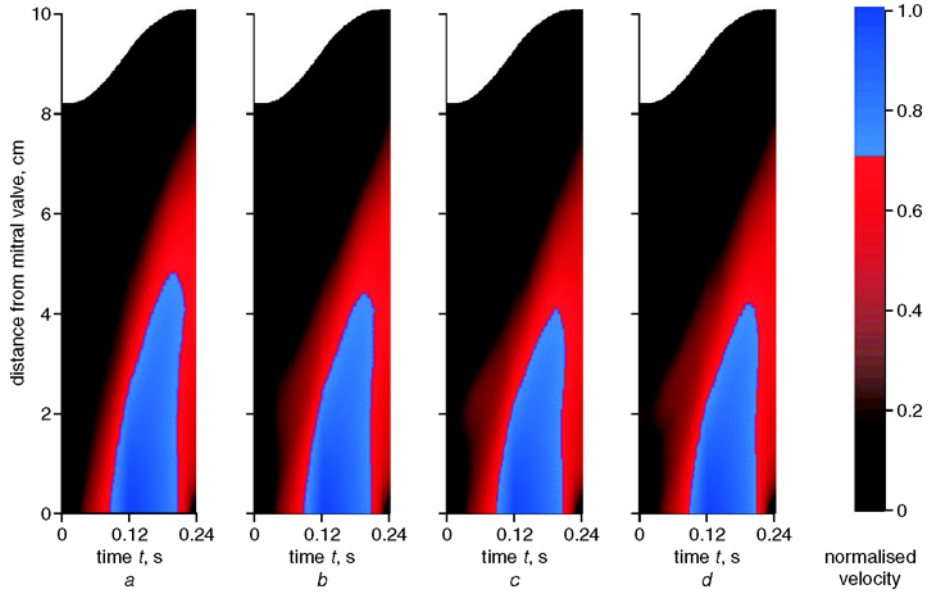

Fig. 7 *Spatiotemporal map of calculated inflow velocity along LV long axis plotted in same manner as CMD echocardiogram. Aliasing limit is set as 70% of spatiotemporal maximum velocity. (a) 1st diastole; (b) 2nd diastole; (c) 3rd diastole; (d) 4th diastole*

the abscissa shows the time elapsed from the onset of diastole of each cardiac cycle. The ordinate shows the distance from the mitral orifice along the LV long axis. The magnitude of the velocity was normalised by the spatiotemporal maximum velocity in each cycle and expressed by a colour according to the scale of the colour bar presented on the right.

The area shown in blue in each map indicates the region where the fluid velocity is greater than 70% of the spatiotemporal maximum velocity in the cardiac cycle. This area is called an aliasing area. Regardless of the presence of flow disturbances in the LV at the onset of diastole, the aliasing area showed a sharply elongated shape, extending almost to the mid-point of the long axis. The propagation velocities (TAKATSUJI *et al.*, 1996), which quantitatively evaluate the degree of sharpness and elongation of the aliasing areas, were 0.58, 0.58, 0.56 and 0.56 $m\,s^{-1}$ for the first–fourth cardiac cycles, respectively.

4 Discussion

4.1 *Adequacy of flow disturbances remaining at beginning of diastole*

Our computer simulation demonstrated that flow disturbances were present in the LV at the onset of diastole. Results showed that the maximum velocity of flow in the LV at that time was approximately 0.45 $m\,s^{-1}$, which was found beneath the mitral valve. KILNER *et al.* (2000) showed a series of magnetic resonance (MR) images of intraventricular flow during a cardiac cycle, where blood flow was visualised by streamlines, and flow velocity was colour-coded. The MR image taken at the beginning of diastole was mostly black because of the low velocity of flow throughout the LV cavity. These *in vivo* data suggested that the present study might have overestimated the intensity of flow disturbances. This overestimation could be attributed to the absence of a phase of isovolumetric relaxation that exists between the end of systole and the onset of diastole in a real heart. Because of this phase, there is hardly any time for intraventricular blood flow to settle down before diastole starts. The brevity of systole may also contribute to an excessive increase in flow velocity: the duration of systole in the present study was 0.24 s, whereas that of a real heart is approximately 0.4 s when the heart rate is 60 beats min^{-1}.

The MR image taken at the end of systole (KILNER *et al.*, 2000) showed that blood inflow from the mitral orifice separated into two streams just above the apical region: one was directed to the anterior wall, and the other was directed to the posterior wall. There was a stagnant flow in the vicinity of a ventricular apex. The results of SABER *et al.* (2003) suggested that it might be a weak vortex rotating counter-clockwise. The flow field obtained at the end of systole in our study was generally similar to those observations. Therefore, although flow disturbances simulated in the present study might be somewhat exaggerated, they were reasonable for discussion of their effect on blood flow during diastole.

4.2 *Effects of remnant flow disturbances on ventricular filling flow at the beginning of diastole*

After the second cardiac cycle, blood flow in the LV at the onset of diastole no longer returned to a quiescent state: a vortical flow existed in the apical region. However, with progress of the ventricular expansion, flow disturbances that existed at the onset of diastole weakened and disappeared. For instance, the vortex present in the vicinity of the ventricular apex at the onset of diastole shrank and moved towards a posterolateral region of the LV. Subsequently, by the end of the acceleration phase, the blood flow pattern in the LV became almost identical to that seen in Figs 5*c* and 6*c* although initial flow disturbances were exaggerated. During the deceleration phase of diastole, the vortex ring was developed through the same process, regardless of the presence of initial flow disturbances. This fact suggests that the effects of initial flow disturbances on a diastolic flow field are fundamentally limited to the acceleration phase of diastole.

4.3 *Effects of remnant flow disturbances on colour M-mode Doppler echocardiogram at the beginning of diastole*

Our computational studies (NAKAMURA *et al.*, 2000; 2003), as well as other numerical (VIERENDEELS *et al.*, 2000; 2002) and experimental (STEEN and STEEN, 1994) studies, have revealed that the size, location and growth speed of an intraventricular diastolic vortex ring are the main determinants of a CMD echocardiogram pattern. As discussed in section 4.2, the effect of the initial flow disturbances on blood flow almost disappeared during the diastole acceleration phase; moreover, flow dynamics during the deceleration phase, especially the vortex ring, were hardly affected. For those reasons, we found almost no change in the CMD echocardiogram patterns and propagation velocity, regardless of the presence of initial flow disturbances. This fact is advantageous from the viewpoint of assessing LV diastolic function.

A CMD echocardiogram obtained by scanning the velocity along the LV long axis during diastole captures features of flow dynamics produced purely by ventricular expansion, because the diastolic CMD echocardiogram pattern is unaffected by initial diastolic flow. Therefore clinical cardiologists can evaluate LV diastolic function independently of LV systolic function using this technique.

Notwithstanding, this also emphasises the limited sensitivity of this method. Even if flow changes in the early stage of diastole exist as a result of some cardiac pathologies, this technique cannot detect them. More sensitive diagnoses that require such flow information are required, necessitating modification of this technique, for instance, by changing the direction of the scanning line along which velocity is measured.

5 Conclusions

Computational fluid dynamics of intraventricular flow were used to investigate the effects of flow disturbances remaining at the beginning of diastole. The following is a summary of those findings:

1) After intraventricular flow becomes cyclically repeatable, initial diastolic flow is not quiescent: flow disturbances, which are actually the remnants of the preceding systolic flow, are present within the LV.

2) The effects of flow disturbances remaining at the onset of diastole on a diastolic flow field are limited to the acceleration phase of diastole. They have hardly any impact on development of the vortex ring in a later stage of diastole.

3) Regardless of the presence of initial flow disturbances, there is almost no variation in the CMD echocardiogram patterns that are evaluated in the same manner as in clinical practice.

4) The CMD echocardiogram obtained by scanning velocity along the LV long axis captures the dynamics of the flow produced purely by a ventricular expansion, with little influence of initial diastolic flow disturbances. This suggests that the CMD technique is suitable to assess LV diastolic function. At the same time, it emphasises the limited sensitivity of this technique.

Acknowledgments—This work was supported by Research Fellowships of the Japan Society for the Promotion of Science for Young

Scientists No. 06787. This study was also funded by ACT-JST ('Research Development for Applying Advanced Computational Science and Technology' of Japan Science and Technology Corporation) 2001–2004 'CREAM—Computational Risk Estimation and Management—in Cardiovascular Clinical Medicine' (Principal Researcher: Takami Yamaguchi).

References

DE MEY, S., DE SUTTER, J., VIERENDEELS, J., and VERDONCK, P. (2001): 'Diastolic filling and pressure imaging: taking advantage of the information in a colour M-mode Doppler image', *Eur. J. Echocardio.*, **12**, pp. 219–233

HONMA, H., OOBAYASHI, K., and UEDA, K. (1998): 'Echographic anatomy for echocardiograms', in: JAPAN MEDICAL ASSOCIATION (Ed.): '*Guide to Echocardiography*' (Nakayama, Tokyo, 1988), pp. 3–16

KITABATAKE, A., INOUE, M., ASAO, M., TANOUCHI, J., MASUYAMA, T., ABE, H., MORITA, H., SENDA, S., and MATSUO, H. (1982): 'Transmitral blood flow reflecting diastolic behavior of the left ventricle in health and disease—a study by pulsed Doppler technique', *Jpn. Circ. J.*, **46**, pp. 92–102

JACOBS, L. E., KOTLER, M. N., and PARRY, W. R. (1990): 'Flow patterns in dilated cardiomyopathy: a pulsed-wave and color flow Doppler study', *J. Am. Soc. Echocardiogr.*, **3**, pp. 294–302

KILNER, P. J., YANG, G. Z., WILKES, A. J., MOHIADDIN, R. H., FIRMIN, D. N., and YACOUB, M. H. (2000): 'Asymmetric redirection of flow through the heart', *Nature*, **404**, pp. 759–761

MOLLER, J. E., SONDERGAARD, E., SEWARD, J. B., APPLETON, C. P., and EGSTRUP, K. (2000): 'Ratio of left ventricular peak E-wave velocity to flow propagation velocity assessed by color m-mode Doppler echocardiography in first myocardial infarction: prognostic and clinical implications', *J. Am. Coll. Cardiol.*, **35**, pp. 363–370

NAKAMURA, M., WADA, S., MIKAMI, T., KITABATAKE, A., and KARINO, T. (2001): 'Relationship between intraventricular flow patterns and the shapes of the aliasing area in color M-mode Doppler echocardiograms—a CFD Study with an axisymmetric model of the LV', *JSME Int. J. Ser. C*, **44**, pp. 1013–1020

NAKAMURA, M., WADA, S., MIKAMI, T., KITABATAKE, A., and KARINO, T. (2002): 'A computational fluid mechanical study on the effects of opening and closing of the mitral orifice on a transmitral flow velocity profile and an early diastolic intraventricular flow', *JSME Int. J. Ser. C*, **45**, pp. 913–922

NAKAMURA, M., WADA, S., MIKAMI, T., KITABATAKE, A., and KARINO, T. (2003) 'Computational study on the evolution of a vortical flow in a human left ventricle during early diastole', *Biomech. Model. Mechanobiol.*, **2**, pp. 59–72

POLEUR, H., HANET, C., GURNE, O., and ROUSSEAU, M. F. (1989): 'Focus on diastolic dysfunction: a new approach to heart failure therapy', *Br. J. Clin. Pharmacol.*, **28**, pp. 41S–52S

SABER, N. R., GOSMAN, A. D., WOOD, N. B., KILNER, P. J., CHARRIER, C. L., and FIRMIN, D. N. (2001): 'Computational flow modeling of the left ventricle based on in vivo MRI data: initial experience', *Ann. Biomed. Eng.*, **29**, pp. 275–283

SABER, N. R., WOOD, N. B., GOSMAN, A. D., MERRIFIELD, R. D., YANG, G. Z., CHARRIER, C. L., GATEHOUSE, P. D., and FIRMIN, D. N. (2003): 'Progress towards patient-specific computational flow modeling of the left heart via combination of magnetic resonance imaging with computational fluid dynamics', *Ann. Biomed. Eng.*, **31**, pp. 42–52

STEEN, T., and STEEN, S. (1994): 'Filling of a model left ventricle studied by colour M mode Doppler', *Cardiovasc. Res.*, **28**, pp. 1821–1827

STUGAARD, M., BRODAHL, U., TORP, H., and IHLEN, H. (1994): 'Abnormalities of left ventricular filling in patients with coronary artery disease: assessment by colour M-mode Doppler technique', *Eur. Heart J.*, **15**, pp. 318–327

TAKATSUJI, H., MIKAMI, T., URASAWA, K., TERANISHI, J., ONOZUKA, H., TAKAGI, C., MAKITA, Y., MATSUO, H., KUSUOKA, H., and KITABATAKE, A. (1996): 'A new approach for evaluation of left ventricular diastolic function: spatial and temporal analysis of left ventricular filling flow propagation by color M-mode Doppler echocardiography', *J. Am. Coll. Cardiol.*, **27**, pp. 365–371

TAYLOR, T. W., and YAMAGUCHI, T. (1995): 'Flow patterns in three-dimensional left ventricular systolic and diastolic flows determined from computational fluid dynamics', *Biorheology*, **32**, pp. 61–71

VIERENDEELS, J. A., RIEMSLAGH, K., DICK, E., and VERDONCK, P. R. (2000): 'Computer simulation of intraventricular flow and pressure gradients during diastole', *J. Biomech. Eng.*, **122**, pp. 667–674

VIERENDEELS, J. A., DICK, E., and VERDONCK, P. R. (2002): 'Hydrodynamics of color M-mode Doppler flow wave propagation velocity v(p): a computer study', *J. Am. Soc. Echocardiogr.*, **15**, pp. 219–224

Authors' biographies

MASANORI NAKAMURA received his PhD in systems and information engineering from Hokkaido University, Japan in 2002. He currently has a postdoctoral position at Tohoku University, supported by JSPS. His main research activity is in the area of computational biomechanics of cardiovascular systems.

SHIGEO WADA received his DEng degree in mechanical engineering from Osaka University, Japan in 1991. He is currently an Associate Professor at the Department of Robotics and Bioengineering in Tohoku University. He has carried out computational studies on blood flow and mass transport in the vascular system.

TAISEI MIKAMI completed medical school at Hokkaido University in 1976 and received his MD in 1985. He is currently an Associate Professor at the School of Medicine in Hokkaido University. His interests include echocardiographic assessments of left ventricular diastolic function.

AKIRA KITABATAKE completed medical school at Osaka University in 1967 and received his MD in 1974. He is currently a Professor at the School of Medicine in Hokkaido University. His main research interest lies in the molecular biological approach to the mechanism of cardiovascular regulation.

TAKESHI KARINO received his PhD from McGill University in 1977. He is currently a Professor at the Research Institute for Electronic Science in Hokkaido University. His research interests have been focused on the elucidation of the localizing mechanisms of atherosclerosis, anastomotic intimal hyperplasia, and cerebral saccular aneurysms.

TAKAMI YAMAGUCHI received his MD from Tokyo Women's Medical College in 1980 and his PhD from University of Tokyo in 1981. He is currently a Professor at the Department of Robotics and Bioengineering in Tohoku University. His current academic interests are focused on the application of computational biomechanics to clinical cardiovascular medicine, and the network and the virtual reality technology applied to medicine.